Optical Materials 60 (2016) 571–576

Contents lists available at ScienceDirect

Optical Materials

journal homepage: www.elsevier.com/locate/optmat

Local-field enhancement of optical nonlinearities in the AGZO nano-triangle array

Hua Long [a], Lijiao Bao [a], Kai Wang [a], Shuhui Liu [b], Bing Wang [a, *]

[a] School of Physics, Huazhong University of Science and Technology, Wuhan 430074, China
[b] Laboratory of Optical Information Technology, Wuhan Institute of Technology, Wuhan 430073, China

ARTICLE INFO

Article history:
Received 12 July 2016
Received in revised form
16 August 2016
Accepted 23 August 2016

Keywords:
AGZO nano-triangle array
Nonlinear optical properties
Local field enhancement
Nanosphere lithography

ABSTRACT

Enhancement of the third order optical nonlinearities in Ga and Al co-doped ZnO (AGZO) nano-triangle array was investigated by performing a Z-scan method with a femtosecond laser (800 nm, 40 fs). The AGZO nano-triangle array was fabricated on silica substrates by nanosphere lithography (NSL) method, showing a surface plasmon resonance (SPR) peak around 3 μm. The two photon absorption (TPA) coefficient and nonlinear refractive index of the AGZO nano-triangle array were determined to be 340 cm/GW and 3.22×10^{-2} cm^2/GW under an excitation intensity of 26 GW/cm^2. It shows a 3.4-fold enhancement of the nonlinear refraction in the AGZO array with respect to that in the AGZO film, which attributes to the local field enhancement effect. The finite-difference time-domain (FDTD) simulation was in agreement with the experimental results. It indicates that the AGZO nano-triangle arrays have potential applications for nonlinear optical devices like all-optical switching, optical limiting and other types of signal processing.

1. Introduction

Nanostructured plasmonic metal systems are known to enhance a variety of optical processes due to the enhanced local electromagnetic field of the metal surface plasmon (SP), including SP enhanced photocatalysis, light-harvesting and photovoltaics, SP enhanced fluorescence and the nonlinear optical properties [1–6]. Recently, metal-oxide nanocrystals and nano-antennas were found to exhibit metallic optical properties and surface plasmon resonance (SPR) peaks in the infrared (IR) region when appropriately doped [7–10]. The doped metal oxide materials show advantage of high transparency in the visible range.

The tuning of localized surface plasmon resonance (LSPRs) in IR region has been demonstrated for a wide variety of doped metal oxide nanoparticles (NPs), such as GZO and ITO. And the surface plasmon enhanced IR spectra and third harmonic generation at resonance wavelength in doped metal oxide nanostructures have been investigated [11–16]. However, the enhanced third order nonlinear optical properties in this kind of materials have not been addressed yet. Our research focus on the enhancement of third-order nonlinear optical properties in Al and Ga co-doped ZnO nano-triangle structures.

As a convenient and low lost method, the method of NSL was combined with pulsed laser deposition (PLD) method to prepare the AGZO nano-triangle arrays. AGZO films were fabricated under exactly the same conditions to compare with the nano-triangle array. Then we investigated the third-order nonlinear optical properties of the AGZO array and the film by Z-scan method, excited by femtosecond lasers at 800 nm. The results show that local field around the AGZO nanostructures can introduce obvious enhance effects on optical nonlinearities. And AGZO nano-triangle arrays show potential applications for nonlinear optical devices.

2. Materials and experiment

The AGZO nano-triangle arrays and films were fabricated on silica substrates (10 mm × 10 mm × 0.3 mm) at room temperature. Firstly, the Ga doped ZnO (GZO) targets (30 mm diameter and 3 mm thick) were fabricated by standard solid-state reaction method. Prescribed amount of ZnO (99.99%) and Ga_2O_3 (99.99%) were mixed and sintered at 1350 °C for 48 h in air atmosphere. The Ga contents in the ceramic targets were 2.93 at%. Then a high purity Al foil of half of the GZO target area was stuck onto the GZO target to form sputtering target. The silica substrates were kept in a mixed

* Corresponding author.
E-mail address: wangbing@hust.edu.cn (B. Wang).

http://dx.doi.org/10.1016/j.optmat.2016.08.022
0925-3467/

solution of H_2SO_4 and H_2O_2 for 1 h at 80 °C, followed by ultrasonic cleaning in another solution of NH_4OH, H_2O_2 and H_2O for one hour to receive a clean and hydrophilic surface.

Secondly, the AGZO nanoparticle arrays were fabricated by NSL and PLD methods. The diameter of the polystyrene (PS) nanospheres used for the preparation of mask (Duke Scientific Corporation) was 820 nm. The silica substrates were ultrasonic cleaned in acetone and alcohol for 5 min respectively. Then the templates for nano-triangle arrays were fabricated on silica substrates by NSL methods. The details for preparing well-ordered PS mask are described in reference [17]. After drying, pulsed laser deposition (PLD) method was used to deposit AGZO on the templets at room-temperature with a Lambda Physik KrF excimer laser (248 nm, 20 ns, 5 Hz) [18,19]. The vacuum chamber was evacuated to 4.5×10^{-3} Pa before the deposition. During the deposition, the oxygen gas was introduced. The oxygen pressure was kept to 0.2 Pa. The energy density at the AGZO target surface was about 2.0 J/cm^2. The deposition time was 60 min. After that, the PS nanospheres were washed away by ultrasonic cleaning in alcohol for about 30 s, leaving behind the AGZO nano-triangle arrays.

Atomic force microscopy (AFM) was used to determine the surface morphology of the nanoparticle arrays. Optical transmittance spectra in the UV–visible range were performed by UV–visible spectrophotometer (HITACHI U3310, with wavelength resolution of 1 nm). The spectra in the infrared range were measured by FTIR (Nexus, with wavenumber resolution of 0.01 cm^{-1}). The third order nonlinear optical properties were determined by Z-scan method excited by femtosecond laser (Coherent, Legend elite, 800 nm, 40 fs, 1 kHz), as reported previously in other reference [17]. The femtosecond laser was focused onto the samples by a lens with 300 mm focal length. The radius of the beam waist (ω_0) is calculated to be about 44 μm. The transmitted beam energy through open aperture (OA) or closed aperture (CA) was detected by photo diode and double-phase lock-in amplifier (SR830, Stanford Research System).

3. Results and discussion

The AFM images of AGZO nano-triangle array were shown in Fig. 1(a)–(c). The surface morphology image in Fig. 1(a) indicates a uniformly distributed nano-triangle array. The edge length of the nano-triangle was about 330 nm. The section analysis image in Fig. 1(b) show that the average height of the nanoparticles with triangular shape was about 60 nm. A 3-D image with larger scanning range was shown in Fig. 1(c).

The transmission spectra in UV–visible range of the AGZO nano-triangle array and film are shown in Fig. 2(a). For the AGZO nano-triangle array and the film the average transmittance in visible range was about 90%. The high transmittance in the visible range indicates low optical loss in the visible range. The optical band energy of the film can be expressed by the following formula [20],

$$\alpha_0 h\nu = C(h\nu - E_g)^2 \quad (1)$$

where α_0 is the linear absorption coefficient, $h\nu$ is the photon energy, C is a constant, and Eg is the optical band gap. The optical band gap can be estimated to be 3.5 eV by extrapolating the linear absorption edge part of the curve, which is similar to the values of GZO and Al doped ZnO (AZO) films reported previously [21].

The FTIR spectra of AGZO nano-triangle array and film were shown in Fig. 2(b). The FTIR transmission spectrum of the array reveal a broad SPR peak in the IR region from 2.4 to 3.6 μm, which is induced by overlap of higher order plasmonic modes as the nanoparticles size increases. Similar results have been reported for

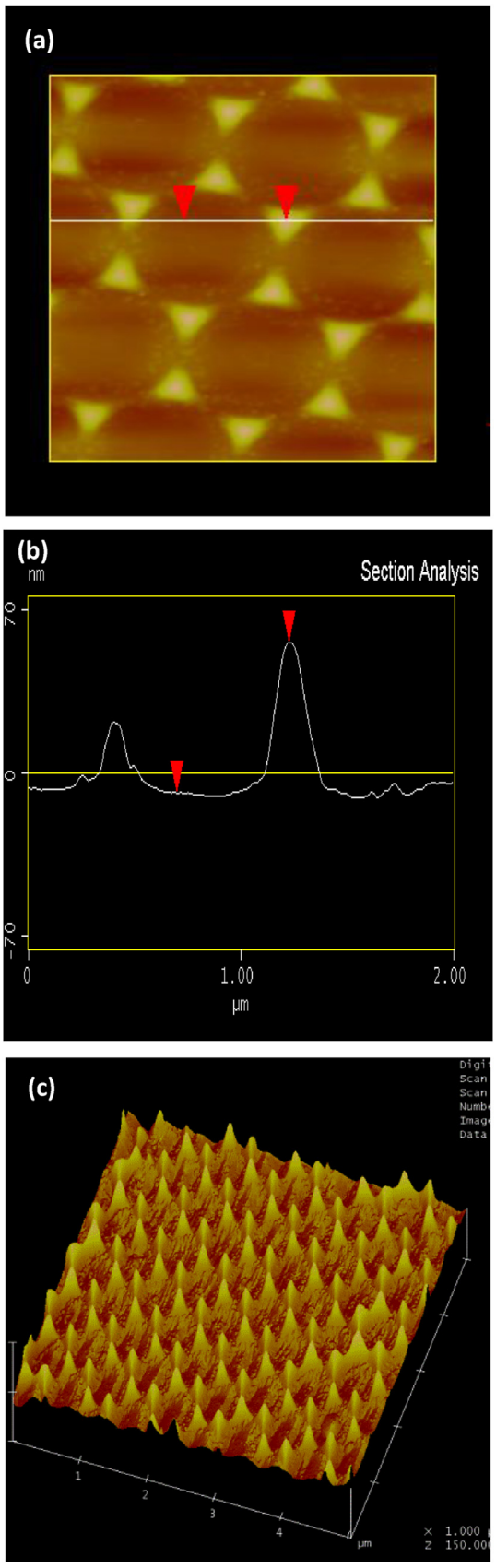

Fig. 1. (a) AFM surface image of the AGZO nano-triangle array, the scan range is 2 μm, (b) AFM section analysis image of the AGZO nano-triangle array, the scale in z axis is 70 nm/div, (c) AFM 3D image of the AGZO nano-triangle array, the scan range is 5 μm.

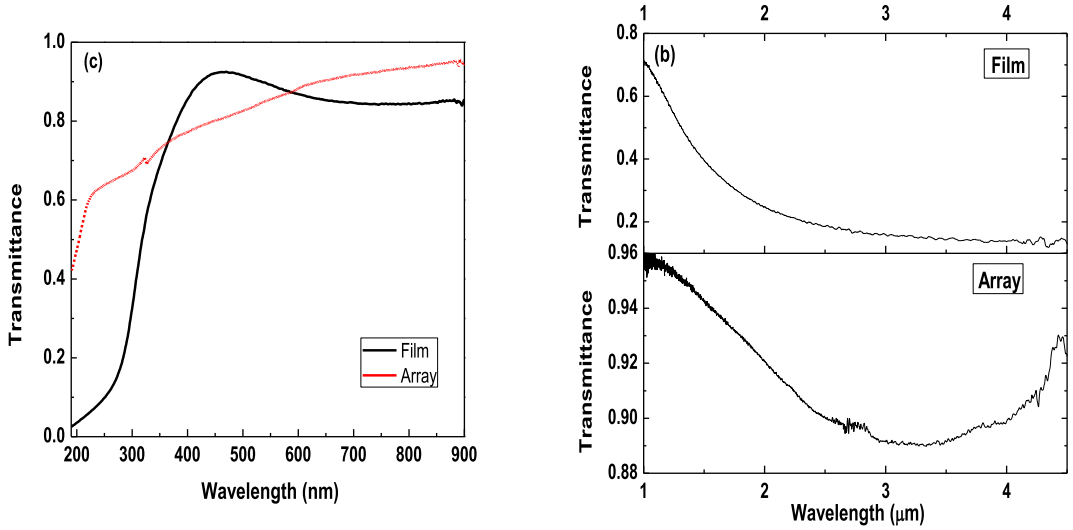

Fig. 2. (a) The transmission spectra of the AGZO array and film in UV–visible region, (b) the FTIR spectra of the AZGO array and film.

AZO and GZO NCs or nanodisks which were prepared by different methods [22–24].

It is known that the metal nano-particles have enhancement effects on the linear and nonlinear optical properties. Similar to this kind of metal materials, the doped metal-oxide nano-particles also show enhancement effects on optical properties. For example, enhancements of IR absorption spectra induced by ITO antennas and GZO nano-arrays have been reported. In order to explore the enhancement effects of the nonlinear optical properties induced by the AGZO nano-triangle arrays, Z-scan method was used to measure the third order nonlinear optical responses of the AGZO arrays excited by 800 nm fs laser. To determine the enhancement effects, the AGZO film with the same contents and 80-nm thickness was fabricated and measured at the same time.

The open-aperture (OA) Z-scan curves of the film and array excited under different laser intensity are presented in Fig. 3(a) and (b), respectively. The laser intensities were 26 GW/cm^2, 84 GW/cm^2, 116 GW/cm^2 and 168 GW/cm^2 at the focal point, respectively. As the laser repetition rate was 1 kHz, the accumulative thermal effects were neglected. The silica substrate was examined under the same condition and no signal has been detected, which exclude the optical nonlinearities from the substrate. To quantify the basic mechanisms responsible (saturable absorption and TPA) for the nonlinear absorption excited by femtosecond lasers, the OA curves are fitted using the following equation [17],

$$dI/dz' = -[\alpha_0/(1 + I/I_s) + \beta I)]I \quad (2)$$

where I is the laser intensity, $z' = z/z_0$, $z_0 = \pi\omega_0^2/\lambda$ is the Rayleigh length, λ is the light wavelength, $\beta = \beta^0/[1 + (I/I_s')]$ is the TPA coefficient, β^0 is the TPA coefficient at low intensity, and I_s and I_s' are the saturation intensity for the saturable absorption (SA) and TPA process, respectively. The results under different excitation intensities could be well fitted with this model.

From Fig. 3(a) and (b), the normalized transmittance signal profiles with a valley at the focal point show obvious TPA processes, which means that in the range of the laser exciting intensity, the mechanism of TPA dominate the nonlinear absorption process. And the OA curves under different excitation intensities could be fitted with the above equation. The fitted results show that the values of *Is* were 100 GW/cm^2 and 200 GW/cm^2 for the film and array, respectively. The values of β were calculated to be 390 cm/GW, 220 cm/GW, 225 cm/GW and 255 cm/GW at different laser intensity. For the array the values were 340 cm/GW, 335 cm/GW,

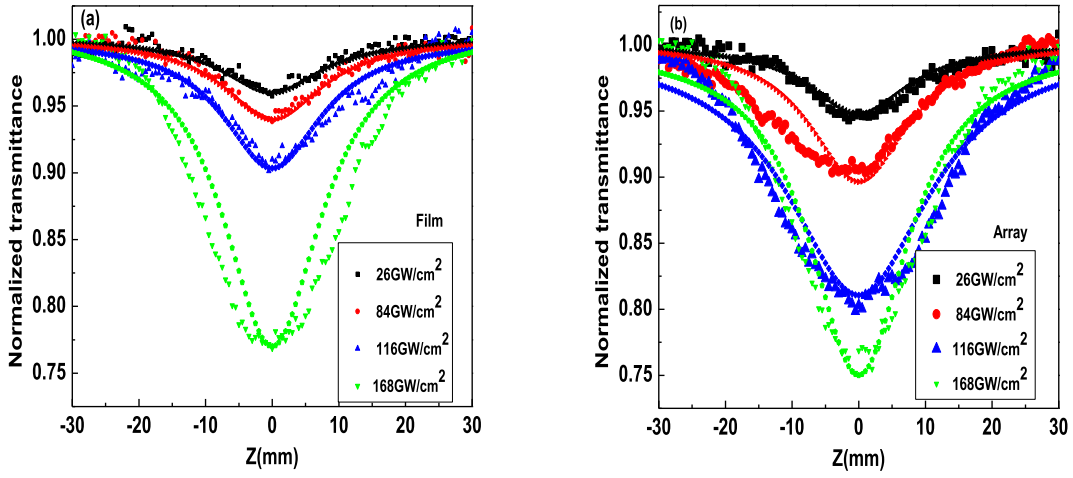

Fig. 3. The OA curves of the AGZO film (a) and nano-triangle array (b), the solid line are the fitted curve.

280 cm/GW and 225 cm/GW, respectively.

The closed aperture (CA) Z-scan curves for AGZO film and nano-triangle array were shown in Fig. 4(a) and (b), respectively. The nonlinear optical refractive index n_2, can be calculated using the following equation [18],

$$n_2 = 1.232\lambda\tau\omega_0^2\Delta T_{p-v}\Big/(1-S)^{0.25}L_{eff}E \quad (3)$$

where τ is the laser pulse width, S is the energy transmittance of the small aperture in CA experiments, and E is the pulse energy at the focal spot.

The valley to peak shape of the CA curves reveals a positive third order nonlinear refractive index at frequencies above the bulk plasmon frequency, consistent with results from earlier studies. The nonlinear refractive index of the nano-triangle array was estimated to be 3.24×10^{-2} cm^2/GW, 2.31×10^{-2} cm^2/GW and 2.0×10^{-2} cm^2/GW as the laser intensity was 26 GW/cm^2, 84 GW/cm^2 and 168 GW/cm^2, respectively. For the film the values of n_2 were 9.44×10^{-3} cm^2/GW, 4.87×10^{-3} cm^2/GW, and 7.3×10^{-3} cm^2/GW, respectively.

Fig. 5(a) shows the intensity-related TPA coefficients of the film and array. From the results, we can see that at low exciting laser intensities which were much lower than I_s (I_s for the film and array were 100 and 200 GW/cm^2, separately.) the TPA dominated the nonlinear absorption process. With the excitation intensity increases, saturable absorption becomes noticeable. Saturable absorption will introduce negative nonlinear absorption coefficient. Then as the excitation intensity increases, the nonlinear absorption coefficient of TPA decreased, indicating a TPA saturation process. The results indicates that the nonlinear absorption coefficient of the nano-triangle array were about the same with that of the film. The values of β decreased when the laser intensity increased to I_s.

Fig. 5(b) shows the intensity-related nonlinear refraction of the film and array. See from the figure, the nonlinear refractive index decreased with the laser intensity increase, which may be induced by the saturable of TPA process in the samples when laser intensity increased. Previous studies of the Kerr nonlinearity of doped metal oxide have identified a relation with a polarization due to free carriers, resulting in a positive n_2. Our experimental results also show positive n_2. Compared with those earlier studies, our current work involves stronger contribution from local electric field. It can be seen that the nonlinear refractive index of the nano-triangle array improved about 3.4 fold than that of the AGZO film.

To evaluate the performance of the arrays for all-optical switching devices, the one-photon figure of merit W, defined by $W = n_2 I_s/\alpha_0\lambda$, and two-photon figure of merit T, defined by $T = \beta\lambda/n_2$, were calculated [25]. To meet the requirements of optical switching devices, the values of W and T should be in the following range $W > 1$ and $T < 1$. Fig. 5(c) and (d) show the intensity-related one-photon and two-photon FOMs, W and **T** of the AGZO nano-triangle array and the film. From the figures, it can be seen that the values of W and T of the arrays can meet the requirement of $T < 1$ and $W > 1$ for all-optical switching devices application. Under low laser intensity, the array will show better nonlinear optical properties. However, the nonlinear optical properties of the AGZO film can't meet the requirements of all-optical switching. So the local-field enhancement on the nonlinear optical properties in the AGZO nano-triangle array is useful for the application of the optical devices. Previous works have report many materials such as Au nanoparticle arrays, RO_2-B_2O_3–SiO_2 (R = Li, Na, and K) polarizing glass containing silver nanorods, double walled carbon nanotubes, have been the candidate for all-optical switching near 800 nm [25–28]. In this paper, the high quality FOMs can be obtained in AGZO nano-triangle array, which is good enough to become a candidate for all-optical switching in infrared region with low loss in visible region.

The local field enhancement effect on the nonlinear optical properties has been reported in some kind of nanostructures, such as porous anodized aluminum oxide nanostructures, Fe_2O_3 hollow nanocrystals, Au nano-particle array/CdTe semiconductor quantum dots hybrid system, and so on [29,30]. However, in our experiments, for the exciting wavelength was in the off-resonance region, the enhancement of nonlinear optical refractive responses should be induced by the local field enhancement near the nano-triangle structures. To characterize the local field enhancement associated with the AGZO nano-triangle array, the FDTD simulations are performed. Fig. 6 shows the schematic diagram of the simulated structure excited by 800 nm light. The parameters of AGZO in FDTD modeling was as the same with parameters in Ref. [31]. And the simulated structure have the same size as the corresponding actual structures. The incident light is normal to the sample surface and the top-down view of the field distribution at the nano-triangle surface of the array is shown in Fig. 6. The highly-concentrated electromagnetic fields can be observed in the edges of nano-triangles, which will lead to the enhancement of nonlinear

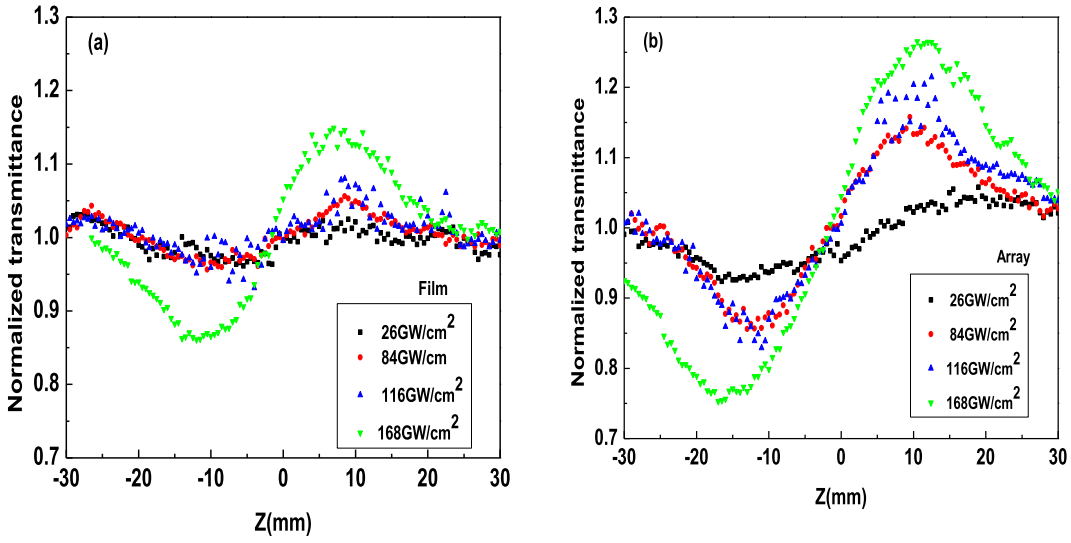

Fig. 4. The CA curves of the AGZO film (a) and nano-triangle array (b).

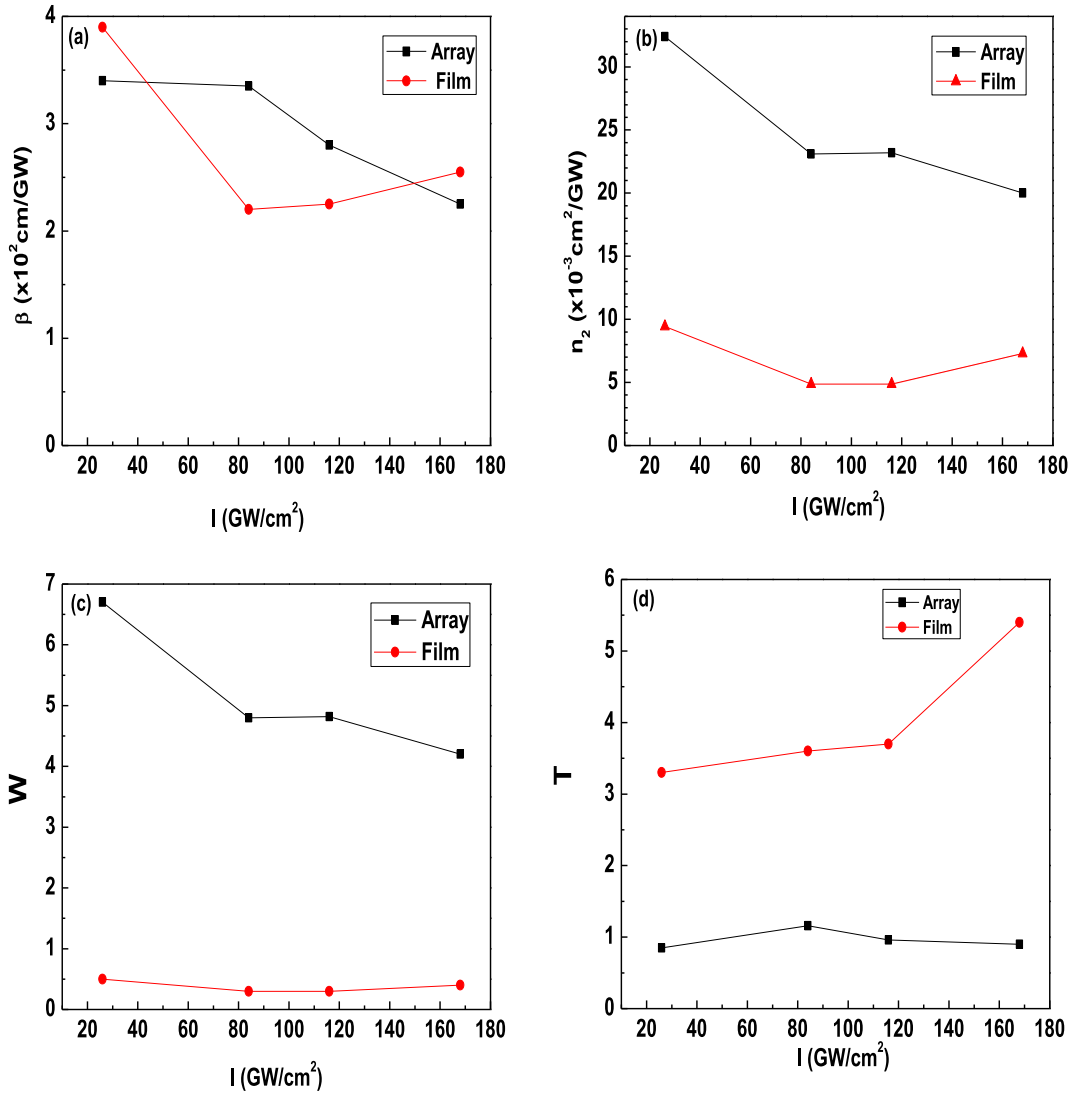

Fig. 5. The intensity related (a) nonlinear absorption coefficients, (b) nonlinear refractive indexes, (c) one-photon FOM, (d) two-photon FOM of the AGZO nano-triangle array and the film.

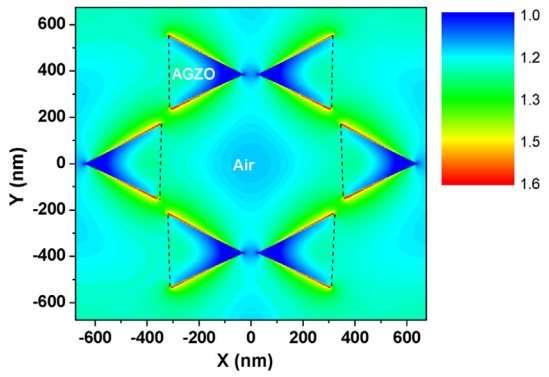

Fig. 6. FDTD simulation showing the electric field intensity distribution in the x-y planes around the AGZO nano-triangle array with edge of 330 nm at 800 nm wavelengths. The polarization of the incident laser is along the x axis.

refractive response in the nanostructures.

The nonlinear Kerr effect was modeled as a change in the refractive index of AGZO, proportional to the product of the third-order susceptibility and the square of the local electric field. A maximum local electric field enhancement of 1.68 is found at the surface of AGZO nano-triangle array, see from Fig. 6. And an averaged local electric field enhancement of 1.2 is found in this simulated x-y plane, which predicts a corresponding enhancement of the nonlinear Kerr effect in the nanostructure. The result is in agreement with the experimental.

The value of the third order nonlinear refractive index of the AGZO array obtained is similar to the value of noble metal nanoparticle arrays. Compared with ZnO film and array, much stronger nonlinear refractive response was observed because no nonlinear refraction in ZnO film [17] and nanoparticle array were observed under the same exciting condition, which may be induced by much higher carrier concentration in the AGZO. And the results were also different from the third-order nonlinear optical properties of Al:ZnO, Mn:ZnO and In:ZnO films excited by nanosecond laser, which show much smaller nonlinear optical refractive index [32,33]. Compared with the films of Al:ZnO and Ga:ZnO, the Al and Ga co-doped ZnO films and arrays fabricated in our experiments show the advantages of larger nonlinear optical refractive index and tuning the third order nonlinear optical properties more

conveniently because the Al doping concentration can be controlled by just changing the Al target area in PLD progress. And compared with metal nano-arrays [25], the AGZO nano-triangle arrays show similar nonlinear optical refractive index values and higher transmission in visible range which means lower optical loss in this range.

4. Conclusions

In conclusion, we have presented and experimentally demonstrated AGZO nano-triangle array exhibiting local-field enhancement on nonlinear optical properties. The highly ordered AGZO nano-triangle arrays were fabricated by NSL and PLD technique, which show high transmittance in the visible region and the SPR peak at wavelength about 3 μm. A significant enhancement of nonlinear refractive index at off-resonance wavelength of the nano-triangle array was observed through Z-scan measurements excited by 800 nm fs laser. It has been shown that non-resonant pumping provides up to about 3.4 times increase of the nonlinear refractive index than the film. The enhancement was attributed to the local field enhancement near the nano-triangle structure. The results indicate that the AGZO nano-triangle arrays have potential applications in nonlinear photonic devices.

Acknowledgment

This work was supported by the National Natural Science Foundation of China under Grant (11004067) and the 973 Programs under grant (2014CB921301). Special thanks to the Analytical and Testing Center of HUST and the Center of Micro-Fabrication and Characterization (CMFC) of WNLO for using their facilities.

References

[1] W.B. Hou, S.B. Cronin, Adv. Funct. Mater. 23 (2013) 1612.
[2] J.H. Song, T. Atay, S. Shi, H. Urabe, A.V. Nurmikko, Nano Lett. 5 (2005) 1557.
[3] S. Linic, P. Christopher, D.B. Ingram, Nat. Mater. 10 (2011) 911.
[4] M.A. Vincenti, M. Grande, G.V. Bianco, D. de Ceglia, T. Stomeo, M. De Vittorio, V. Petruzzelli, G. Bruno, A. D'Orazio, M. Scalora, J. Appl. Phys. 113 (2013) 013103.
[5] H.B. Hu, K. Wang, H. Long, W.W. Liu, B. Wang, P.X. Lu, Nano Lett. 15 (2015) 3351.
[6] N. Mattiucci, G. D'Aguanno, H.O. Everitt, J.V. Foreman, J.M. Callahan, M.C. Buncick, J. Bloemer, Opt. Express 20 (2012) 1868.
[7] G. Garcia, R. Buonsanti, A. Llordes, E.L. Runnerstrom, A. Bergerud, D.J. Milliron, Adv. Opt. Mater. 1 (2013) 215.
[8] A. Comin, L. Manna, Chem. Soc. Rev. 43 (2014) 3957.
[9] A.M. Schimpf, N. Thakkar, C.E. Gunthardt, D.J. Masiello, D.R. Gamelin, ACS Nano 8 (2014) 1065.
[10] D.B. Tice, S.Q. Li, M. Tagliazucchi, D.B. Buchholz, E.A. Weiss, R.P.H. Chang, Nano Lett. 14 (2014) 1120.
[11] M. Caldarola, P. Albella, E. Cortés, M. Rahmani, T. Roschuk, G. Grinblat, R.F. Oulton, A.V. Bragas, S.A. Maier, Nat. Commun. 6 (2015) 7915.
[12] B. Metzger, M. Hentschel, T. Schumacher, M. Lippitz, X.C. Ye, C.B. Murray, B. Knabe, K. Buse, H. Giessen, Nano Lett. 14 (2014) 2867.
[13] M. Abb, Y.D. Wang, N. Papasimakis, C.H. de Groot, O.L. Muskens, Nano Lett. 14 (2014) 346.
[14] S.L. Ke, B. Wang, H. Huang, H. Long, K. Wang, P.X. Lu, Opt. Express 23 (2015) 008888.
[15] M. Abb, Y.D. Wang, C.H. de Groot, O.L. Muskens, Nat. Commun. 5 (2014) 4869.
[16] I.V. Kityk, N.S. AlZayed, K. Kobayashi, X.M. Chen, M. Oyama, A.M. El-Naggar, A.A. Albassam, Phys. E 71 (2015) 91.
[17] L.C. Zhang, G. Yang, K. Wang, M. Fu, Y. Wang, H. Long, P.X. Lu, Opt. Commun. 291 (2013) 395.
[18] H. Long, M. Fu, Y.H. Li, Thin Solid Films 519 (2010) 1346.
[19] H. Long, A.P. Chen, G. Yang, J. Inorg. Mater. 24 (2009) 221.
[20] Y. Natsume, H. Sakata, Thin Solid Films 372 (2000) 30.
[21] E.D. Gaspera, M. Bersani, M. Cittadini, M. Guglielmi, D. Pagani, R. Noriega, S. Mehra, A. Salleo, A. Martucci, J. Am. Chem. Soc. 135 (2013) 3439.
[22] A.M. Schimpf, C.E. Gunthardt, J.D. Rinehart, J.M. Mayer, D.R. Gamelin, J. Am. Chem. Soc. 135 (2013) 16569.
[23] J. Kim, G.V. Naik, N.K. Emani, IEEE J. Sel. Top. Quant. 19 (2013) 4601907.
[24] R. Buonsanti, A. Llordes, S. Aloni, B.A. Helms, D.J. Milliron, Nano Lett. 11 (2011) 4706.
[25] K. Wang, H. Long, M. Fu, G. Yang, P.X. Lu, Opt. Express 18 (2010) 13874.
[26] Q.Q. Wang, J.B. Han, H.M. Gong, D.J. Chen, X.J. Zhao, J.Y. Feng, J.J. Ren, Adv. Funct. Mater. 16 (2006) 2405.
[27] N. Kamaraju, S. Kumar, B. Karthikeyan, A. Moravsky, R.O. Loutfy, A.K. Sood, Appl. Phys. Lett. 93 (2008) 091903.
[28] N. Kamaraju, S. Kumar, Y.A. Kim, T. Hayashi, H. Muramatsu, M. Endo, A.K. Sood, Appl. Phys. Lett. 95 (2009) 081106.
[29] H.M. Fan, G.J. You, Y. Li, Z. Zheng, H.R. Tan, Z.X. Shen, S.H. Tang, Y.P. Feng, J. Phys. Chem. C 113 (2009) 9928.
[30] M. Fu, K. Wang, H. Long, G. Yang, P.X. Lu, F. Hetsch, A.S. Susha, A.L. Rogach, Appl. Phys. Lett. 100 (2012) 063117.
[31] J. Kim, G.V. Naik, A.V. Gavrilenko, K. Dondapati, V.I. Gavrilenko, S.M. Prokes, O.J. Glembocki, V.M. Shalaev, A. Boltasseva, Phys. Rev. X 3 (2013) 041037.
[32] M.Y. Tan, C.B. Yao, X.Y. Yan, J. Li, S.Y. Qu, J.Y. Hu, W.J. Sun, Q.H. Li, S.B. Yang, Opt. Mater. 51 (2016) 133–138.
[33] Z.M. Htwe, Y.D. Zhang, C.B. Yao, H. Li, H.Y. Li, P. Yuan, Opt. Mater. 52 (2016) 6–13.